



Quantitative studies on structure–ORAC relationships of anthocyanins from eggplant and radish using 3D-QSAR



Pu Jing^{a,*}, Shujuan Zhao^{a,b,1}, Siyu Ruan^b, Zhongquan Sui^a, Lihong Chen^b, Linlei Jiang^a, Bingjun Qian^{a,*}

^a Research Center for Food Safety and Nutrition, Key Lab of Urban Agriculture (South), Bor S. LUH Food Safety Research Center, School of Agriculture & Biology, Shanghai Jiao Tong University, Shanghai 200240, China

^b Department of Food Science and Engineering, School of Food and Biological Engineering, Jiangsu University, Jiangsu 212013, China

ARTICLE INFO

Article history:

Received 16 April 2013

Received in revised form 16 August 2013

Accepted 19 August 2013

Available online 29 August 2013

Keywords:

3D-QSAR
Anthocyanins
Oxygen radical
Structure
CoMFA
CoMSIA

ABSTRACT

The 3-dimensional quantitative structure activity relationship (3D-QSAR) models were established from 21 anthocyanins based on their oxygen radical absorbing capacity (ORAC) and were applied to predict anthocyanins in eggplant and radish for their ORAC values. The cross-validated $q^2 = 0.857/0.729$, non-cross-validated $r^2 = 0.958/0.856$, standard error of estimate = 0.153/0.134, and $F = 73.267/19.247$ were for the best QSAR (CoMFA/CoMSIA) models, where the correlation coefficient $r^2_{\text{pred}} = 0.998/0.997$ (>0.6) indicated a high predictive ability for each. Additionally, the contour map results suggested that structural characteristics of anthocyanins favourable for the high ORAC. Four anthocyanins from eggplant and radish have been screened based on the QSAR models. Pelargonidin-3-[(6''-p-coumaroyl)-glucosyl(2→1)glucoside]-5-(6''-malonyl)-glucoside, delphinidin-3-rutinoside-5-glucoside, and delphinidin-3-[(4''-p-coumaroyl)-rhamnosyl(1→6)glucoside]-5-glucoside potential with high ORAC based the QSAR models were isolated and also confirmed for their relative high antioxidant ability, which might attribute to the bulky and/or electron-donating substituent at the 3-position in the C ring or/and hydrogen bond donor group/electron donating group on the R₁ position in the B ring.

© 2013 Elsevier Ltd. All rights reserved.

1. Introduction

Anthocyanins belong to the widespread class of flavonoid compounds and are considered as natural, water-soluble, nontoxic pigments (Kong, Chia, Goh, Chia, & Brouillard, 2003). Researches on anthocyanins were carried out because of their biological and pharmacological properties, especially antioxidant activity (Kahkonen & Heinonen, 2003).

The relationship between anthocyanin structure and antioxidant capacity has been studied. The number and position of hydroxylation and methoxylation in the B ring is commonly regarded as important for the radical scavenging activities of anthocyanins (Kahkonen & Heinonen, 2003; Noda, Kneyuki, Igarashi, Mori, & Packer, 2000; Wang, Cao, & Prior, 1997). Delphinidin containing three hydroxylation in the B ring showed a higher antioxidant activity among the six common anthocyanidins (Kahkonen

& Heinonen, 2003; Noda et al., 2000) whereas the pelargonin had the lowest antioxidant activity (Wang et al., 1997). Anthocyanin glycosylation patterns affected the total antioxidant capacity (Azuma et al., 2008; Bao, Cai, Sun, Wang, & Corke, 2005; Rahman, Ichianagi, Komiyama, Hatano, & Konishi, 2006; Rice-Evans, Miller, & Paganga, 1996; Seeram & Nair, 2002; Wang et al., 1997, 1999; Yoshiki, Okubo, & Igarashi, 1995). A general trend of decreasing TEAC by glycosylation was observed (Rice-Evans et al., 1996). However, glycosylation at C-3 and C-5 of the anthocyanin skeleton have shown an enhancing effect in the chemiluminescence intensity (lipid peroxidation) (Yoshiki et al., 1995). Different sugars may have different effects on the antioxidant activity of an anthocyanin (Wang et al., 1997). Depending on anthocyanidins, different glycosylation patterns either enhanced or reduced the antioxidant power (Kahkonen & Heinonen, 2003). Additional hydroxylation in delphinidin did not increase the Trolox equivalent antioxidant capacity in ORAC assay (Wang et al., 1997) but increased the chemiluminescence intensity in the chemiluminescence assay (Yoshiki et al., 1995) compared to cyanidin. Delphinidin derivatives acylated with caffeic acid showed a higher antioxidant activity than the deacylated corresponding (Azuma et al., 2008).

More recently quantitative structure activity relationship (QSAR) studies have served as an efficient tool to elucidate the structure–activity relationships of antioxidants (Jing et al., 2012;

Abbreviations: 3D-QSAR, 3-dimensional quantitative structure activity relationship; ORAC, oxygen radical absorbing capacity; CoMFA, comparative molecular field analysis; CoMSIA, molecular similarity indices analysis; LOO, Leave-One-Out; TEAC, trolox equivalent antioxidant capacity.

* Corresponding authors. Tel./fax: +86 21 3420 7074.

E-mail addresses: pjcolumbus@gmail.com (P. Jing), bjqianfd@sytu.edu.cn (B. Qian).

¹ These authors contributed equally to this work.

Vajragupta, Boonchoong, & Wongkrajang, 2000; Yamagami, Akamatsu, Motohashi, Hamada, & Tanahashi, 2005). This study aimed to build the QSAR models of the anthocyanins using the comparative molecular field analysis (CoMFA) and the comparative molecular similarity indices analysis (CoMSIA) methods to predict eggplant/radish anthocyanins potential with high oxygen radical absorbance capacity and also understand their quantitative structure–activity relationships. The study should provide an efficient tool to screen anthocyanins from natural sources for a high bioactivity. Then target anthocyanins could be directly isolated for further experiment evaluation. Additionally structure criteria of anthocyanins for a high ORAC were also explored.

2. Materials and methods

2.1. Chemicals

Cyanidin, delphinidin, pelargonidin 3-glucoside, cyanidin 3-glucoside, cyanidin 3-galactoside, cyanidin 3-rutinoside, cyanidin 3-sophoroside, cyanidin 3,5-diglucoside, delphinidin 3,5-diglucoside, pelargonidin 3,5-diglucoside and cyanidin 3-O-β-(6''-p-coumaroyl-sambubioside)-5-glucoside were purchased from Polyphenols (Sandnes, Norway). Delphinidin 3-sambubioside, delphinidin 3-rutinoside, delphinidin 3-glucoside, cyanidin 3-arabinoside were purchased from Phytolab (Vestenbergsgreuth, German). Pelargonidin was purchased from Chromadex (Santa Ana, CA, USA). All other chemicals were purchased from Sigma–Aldrich (Shanghai, China).

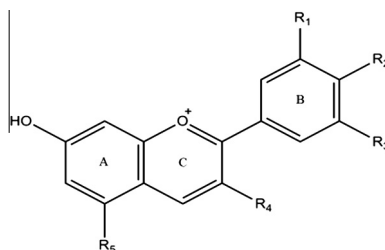
2.2. Experimental design

Common anthocyanins were randomly selected for the study. The 3D-QSAR models were established from the data set of 21 anthocyanins (Table 1). The experimental biological activity values were measures of Trolox equivalent antioxidant capacity (TEAC) for ORAC. The QSAR models were established by comparative field analysis (CoMFA, SYBYL-X 1.2) and comparative molecular similarity index analysis (CoMSIA, SYBYL-X 1.2). The critical structural characteristics of anthocyanins associated with free oxygen radical scavenging activities were analysed. Four anthocyanins in eggplant and radish were randomly chosen for their ORAC calculation in established QSAR models. Three among them were isolated from eggplant and radish and evaluated experimentally at 20 μmol/L were prepared for the antioxidant capacity.

2.3. Oxygen radical absorbance capacity (ORAC) assay

The determination of oxygen radical absorbing capacity of the studied compounds was performed according to the previously reported procedure (Moore et al., 2005) in a Synergy 2 Multi-Mode Microplate Reader (BioTek, Winooski, VT, USA). Samples and Trolox standards were prepared with 50% acetone. All other reagents were prepared in 75 mmol/L phosphate buffer (pH 7.4). Briefly, each well in 96-well plate contained 30 μL of 20 μmol/L sample or 50% acetone for blank and 225 μL fluorescein (81.63 nmol/L). The plate with cover was incubated for 20 min in 37 °C, and then 25 μL AAPH (0.36 mol/L) were added to each well to start reaction,

Table 1
Chemical structure and oxygen radical absorbance capacity of anthocyanins.



Compounds	R ₁	R ₂	R ₃	R ₄	R ₅	Experimental TEAC	Predicted TEAC	
							CoMFA	CoMSIA
1	OH	OH	H	OH	OH	6.764	5.978	6.372
2	H	OH	H	OH	OH	5.801	6.068	5.276
3	OH	OH	OH	OH	OH	3.084	2.689	2.725
4	OH	OH	H	O-glc	OH	4.723	5.347	6.454
5	H	OH	H	O-glc	OH	6.309	6.721	6.754
6	OH	OH	OH	O-glc	OH	5.137	4.420	4.435
7 ^a	OH	OH	H	O-gal	OH	9.608	9.375	8.595
8	OH	OH	H	O-ara	OH	1.286	1.768	2.696
9	OH	OH	H	O-rut	OH	5.940	5.954	5.108
10	OH	OH	H	O-sop	OH	5.809	6.291	5.725
11	OH	OH	OH	O-rut	OH	4.098	3.673	4.141
12	OH	OH	OH	O-sam	OH	5.101	4.707	4.957
13	OH	OH	H	O-glc	O-glc	4.468	4.225	4.991
14	H	OH	H	O-glc	O-glc	5.808	5.608	5.901
15	OH	OH	OH	O-glc	O-glc	3.223	3.496	3.574
16	OH	OH	H	O-cou-sam	O-glc	8.620	8.193	8.597
17	OCH ₃	OH	H	O-glc	OH	5.178	5.116	5.084
18	OCH ₃	OH	H	O-gal	OH	2.615	2.980	2.490
19	OCH ₃	OH	OCH ₃	O-glc	OH	2.916	2.718	2.295
20	OCH ₃	OH	H	O-ara	OH	4.070	4.134	3.844
21	OCH ₃	OH	OCH ₃	O-glc	O-glc	4.099	3.895	3.897

glc, glucoside; gal, galactose; ara, arabinose; rut, rutinose; sop, sophoroside; sam, sambubioside; cou-sam, sambubioside acylated with *p*-coumaric acid; cou-rut, rutinose acylated with *p*-coumaric acid; cou-sop, sophoroside acylated with *p*-coumaric acid; mal-glc, glycoside acylated with malonic acid.

^a Compound for the template alignment.

resulting in a final total volume of 280 μL . The fluorescence was recorded every minute for 2 h at 37 $^{\circ}\text{C}$, where excitation and emission wavelengths were 485 and 528 nm. Standards and samples were performed in triplicate. Trolox equivalents were calculated using the relative area under the curve for samples compared to a Trolox standard curve prepared under the same experimental conditions. Results are expressed as micromoles of Trolox equivalents per micromole of anthocyanins.

2.4. Molecular modelling and alignment

Molecular structure building was accomplished using the molecular modelling program from the SYBYL-X 1.2 software (Tripos, St. Louis MO, USA) on a Windows operation system. The energy minimisations of each structure were conducted with the Powell method using the Tripos force field (Clark, Cramer, & Vanopdenbosch, 1989), where a convergence criterion of 0.005 kcal/(mol \AA) was used as the termination of the Powell conjugate gradient algorithm and the maximum iterations were set to 1000 steps. The partial atomic charges were calculated using the Gasteiger–Hückle method. Other parameters were default. Molecular superimposition of anthocyanins in the training set (Table 1) on the template structure was performed by database alignment method in SYBYL. The most active compound 7 was chosen as a template for superimposition and the common structure was the A and C rings, assuming that its conformation represented the most bioactive conformation of the anthocyanins. Fig. 1 shows the 3D-view of 21 aligned molecules.

2.5. Comparative molecular field analysis (CoMFA) and comparative molecular similarity index analysis (CoMSIA)

Comparative molecular field analysis (CoMFA) and comparative molecular similarity index analysis (CoMSIA) are 3D-QSAR methods that apply statistical correlation techniques to analyse the quantitative relationship between the biological activity for a set of compounds with a special alignment, and their three-dimensional electronic, steric properties, plus hydrogen bond donor/acceptor and hydrophobic properties specifically for CoMSIA. In this study, CoMFA was started with the QSAR option of SYBYL-X 1.2 in the Tripos force field (Cramer, Patterson, & Bunce, 1988). A 3D cubic lattice with a grid spacing of 2 \AA in x , y , and z directions was created to encompass the aligned molecules in order to obtain the CoMFA and CoMSIA descriptor fields. The energies of steric (Lennard–Jones potential) and electronic (Coulomb potential)

fields were calculated using a sp^3 carbon atom as the steric probe atom and a +1 charge for the electrostatic probe. The cutoff value for both steric and electrostatic interactions was set at 30.0 kcal/mol. In CoMSIA analysis (Klebe & Abraham, 1999), steric, electrostatic, hydrophobic, hydrogen bond donor and hydrogen bond acceptor properties were evaluated. Gaussian-type distance dependence was used to calculate the similarity indices. The default attenuation factor ($\alpha = 0.3$) was used. There were no cutoff limits in CoMSIA analysis.

2.6. Partial least square (PLS) analysis

The method of partial least square (PLS) implemented in the QSAR module of SYBYL was used to construct and validate the models. The CoMFA and CoMSIA descriptors were used as independent variables, and the biological activities in TEAC values were used as dependent variables in PLS regression analysis to derive 3D-QSAR models using the standard implementation in the SYBYL-X 1.2 package (Bush & Nachbar, 1993). The Leave-One-Out (LOO) was performed to obtain the optimum number of components, which consequently was used to develop the final non-cross-validated model determined by the cross-validation coefficient q^2 , the non-cross-validated coefficient r^2 and its standard error s and F -test values for the model evaluation. To further assess the robustness and statistical confidence of the derived QSAR models, bootstrap analysis for 10 runs was performed. CoMFA and CoMSIA contour maps that intuitively reflect and analyse the different field effects on the activity (Zhang et al., 2011) were obtained by interpolation of the pair-wise products between the PLS coefficients and the standard deviations of the corresponding CoMFA or CoMSIA descriptor values.

2.7. Extraction and purification of anthocyanins

Extraction and purification of eggplant anthocyanins were performed according to the method of Ichyanagi et al. (2005). Purple eggplants (5 kg) and red radishes (5 kg) were purchased from a local market. The peel of the eggplant or radish roots was immersed in 10 L of methanol containing 0.01% HCl and extracting for 2 h. Extracts were evaporated to dryness under vacuum condition at 40 $^{\circ}\text{C}$. The residue was dissolved in distilled water and applied to a 600 cm \times 50 cm Amberlite XAD-7HP column (Huideyi, Beijing, China). The column was well washed with distilled water containing 0.01% HCl to remove water-soluble compounds, and then the anthocyanin fraction was eluted with methanol containing 0.01% HCl and collected. The methanol was removed from the anthocyanin fraction under vacuum conditions at 40 $^{\circ}\text{C}$. The anthocyanins aqueous solution was applied onto a 100 cm \times 2.5 cm open column packed with Sephadex LH-20 (Huideyi, Beijing, China) and separated by 50% aqueous methanol containing 0.01% HCl. Anthocyanin fractions were further purified in an Agilent preparative HPLC system equipped with a semi-preparative ZORBAX Eclipse XDB-C18 column (5 μm particle size, 250 mm \times 9.4 mm id; Agilent, USA). Anthocyanin peak fractions were collected and evaporated to dryness in a nitrogen-blow. Pelargonidin-3-[(6'-*p*-coumaroyl)-glucosyl(2 \rightarrow 1)glucoside]-5-(6''-malonyl)-glucoside from red radish roots, and delphinidin-3-[(4''-*p*-coumaroyl)-rhamnosyl(1 \rightarrow 6)glucoside]-5-glucoside from eggplant peel were obtained.

The delphinidin-3-rutinoside-5-glucoside was obtained by alkaline hydrolysis of eggplant anthocyanins according to a previous method (Durst & Wrolstad, 2001). Anthocyanin-rich extracts from eggplant peels were saponified in a screw-up test tube with 10 mL of 10% aqueous KOH for 8 min at room temperature in the dark. Then the solution was neutralised and acidified by HCl (2 mol/L). The hydrolysate was purified according to the above

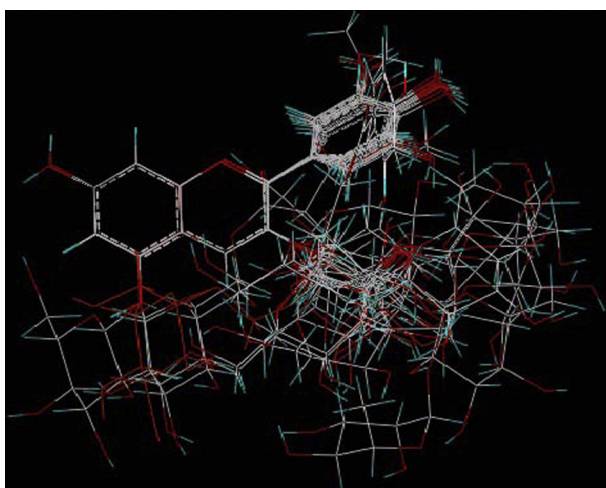


Fig. 1. Alignment of the compounds used in the training set.

Table 2
Statistical parameters of the CoMFA and CoMSIA models.

	CoMFA	CoMSIA	Validation criteria (Golbraikh & Tropsha, 2002))
<i>Statistics parameters</i>			
q^2	0.857	0.729	>0.6
r^2	0.958	0.856	>0.8
s	0.153	0.134	
F	73.267	19.247	
PLS component	4	4	
<i>Field contribution</i>			
Steric	0.734	0.096	
Electrostatic	0.266	0.206	
Hydrophobic		0.206	
H-bond donor		0.240	
H-bond acceptor		0.254	
r^2_{bs} (10 runs)	0.902	0.906	
SD_{bs}	0.068	0.042	
r^2_{pred}	0.998	0.997	>0.6
r_0^2	0.958	0.941	
k	0.956	0.932	$0.85 \leq k \leq 1.15$
$(r^2_{pred} - r_0^2) / r^2_{pred}$	0.042	0.057	<0.1

q^2 , cross-validated correlation coefficient after the Leave-One-Out procedure; r^2 , non-cross-validated correlation coefficient; s , standard error of estimate; F , F -test value; PLS component, optimum number of components; r^2_{bs} , bootstrapping correlation; SD_{bs} , bootstrapping standard deviation; r^2_{pred} , correlation coefficient for test set predictions; r_0^2 , correlation coefficient for the regression through origin for experimental versus predicted activities; k , slope for regression through origin from experimental versus predicted.

procedure as same as the above. Delphinidin-3-rutinoside-5-glucoside was obtained from eggplant peel after alkaline hydrolysis and following purification.

All purified anthocyanins from eggplant and radish roots were identified by LC-MS and ^1H -, ^{13}C -NMR spectrometry (Supplementary Data). The purity (HPLC) is >96%.

3. Results and discussion

3.1. CoMFA and CoMSIA models

The statistic results for both CoMFA and CoMSIA models are shown in Table 2. The internal validation of LOO cross-validated q^2 and non-cross validated coefficient r^2 are commonly applied as a criterion of robustness and predictive ability of a QSAR model. The commonly accepted values for a satisfactory QSAR model and $q^2 > 0.5$ and $r^2 > 0.8$ (Golbraikh & Tropsha, 2002). A highly predictive CoMFA model with LOO cross-validated q^2 of 0.857 and correlation value r^2 of 0.958 was obtained. The steric contribution and

electrostatic contribution were 73.4% and 26.6% for the QSAR model. The standard error of estimate and F -test value were 0.153 and 73.267, respectively. The yielded r^2_{bs} value 0.902 for CoMFA ($SD_{bs} = 0.068$) validated further the developed models.

The statistical results of the best CoMSIA model are also listed in Table 2. The good cross-validated q^2 of 0.729 (>0.5) and the non-cross-validated coefficient r^2 of 0.856 (>0.8) were obtained based on the steric, electrostatic, H-bond donor/acceptor, and hydrophobic fields that explained 9.6, 20.6, 20.6, 24.0 and 25.4% of the variance from the QSAR model, respectively. The non-cross-validated coefficient s and F value are 0.134 and 19.247, respectively. The yielded r^2_{bs} value 0.906 for CoMSIA ($SD_{bs} = 0.042$) further supports the statistical validity of the developed CoMSIA models. The predictive ability of the models was validated with the correlation coefficient $r^2_{pred} = 0.998/0.997$ (>0.6) for each models, indicating that both CoMFA and CoMSIA models should have high predictive abilities for oxygen radical absorbance capacity of anthocyanins. The experimental and predicted activities in the training set are shown in Table 1. The values of correlation coefficient r^2_{pred} , $[(r^2_{pred} - r_0^2) / r^2_{pred}]$, and k of CoMFA and CoMSIA models satisfy the criteria in Table 2.

3.2. CoMFA and CoMSIA contour maps analysis

CoMFA and CoMSIA contour maps analyses were performed to visualise the important regions in 3D molecules where the steric, electrostatic, hydrogen-bond donor/acceptor, and hydrophobic fields may affect the oxygen radical absorbing capacity of the studied compounds. The weight of $\text{StDev} \times \text{Coeff}$ was used to calculate field energies for all fields in CoMFA and CoMSIA models. The highly active compound 7 was shown as the template ligand for all contour map positions.

3.3. CoMFA contour maps

The steric contour map with sterically favourable (marked in green) and sterically unfavourable (marked in yellow) regions is shown in Fig. 2a. Large green contours are located around the R_4 of C ring and the R_1 of B ring, indicating that the more bulky substituent at those locations appeared to be favourable for the ORAC of anthocyanins. These functional structural properties could explain oxygen radical absorbance capacity of most anthocyanins in Table 1. For instance, compound 6 (R_1, R_2, R_3 : OH, R_4 : Glc, R_5 : H, TEAC = 5.137) with a glycosylation on the 3-position in the C ring, had a higher activity than the corresponding compound 3 (R_1, R_2, R_3 : OH, R_4 : H, R_5 : H, TEAC = 3.084) without a bulky group at the same position. Compound 1 (R_1, R_2 : OH, R_3 : H, R_4 : H, R_5 : H,

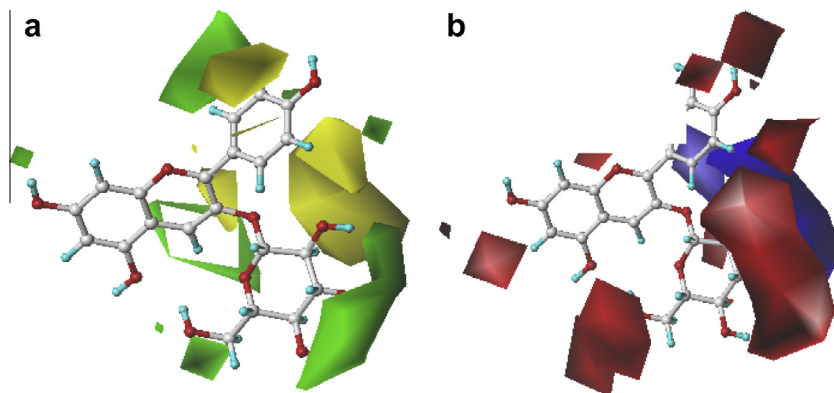


Fig. 2. CoMFA contour maps. (a) steric contour map: the green is sterically favored for the activity, whereas the yellow is unfavourable; (b) electrostatic contour map: the blue contour for positive-charged substituent is favourable, whereas the red contour for the negative-charged substituent is favourable. (For interpretation of the references to colour in this figure legend, the reader is referred to the web version of this article.)

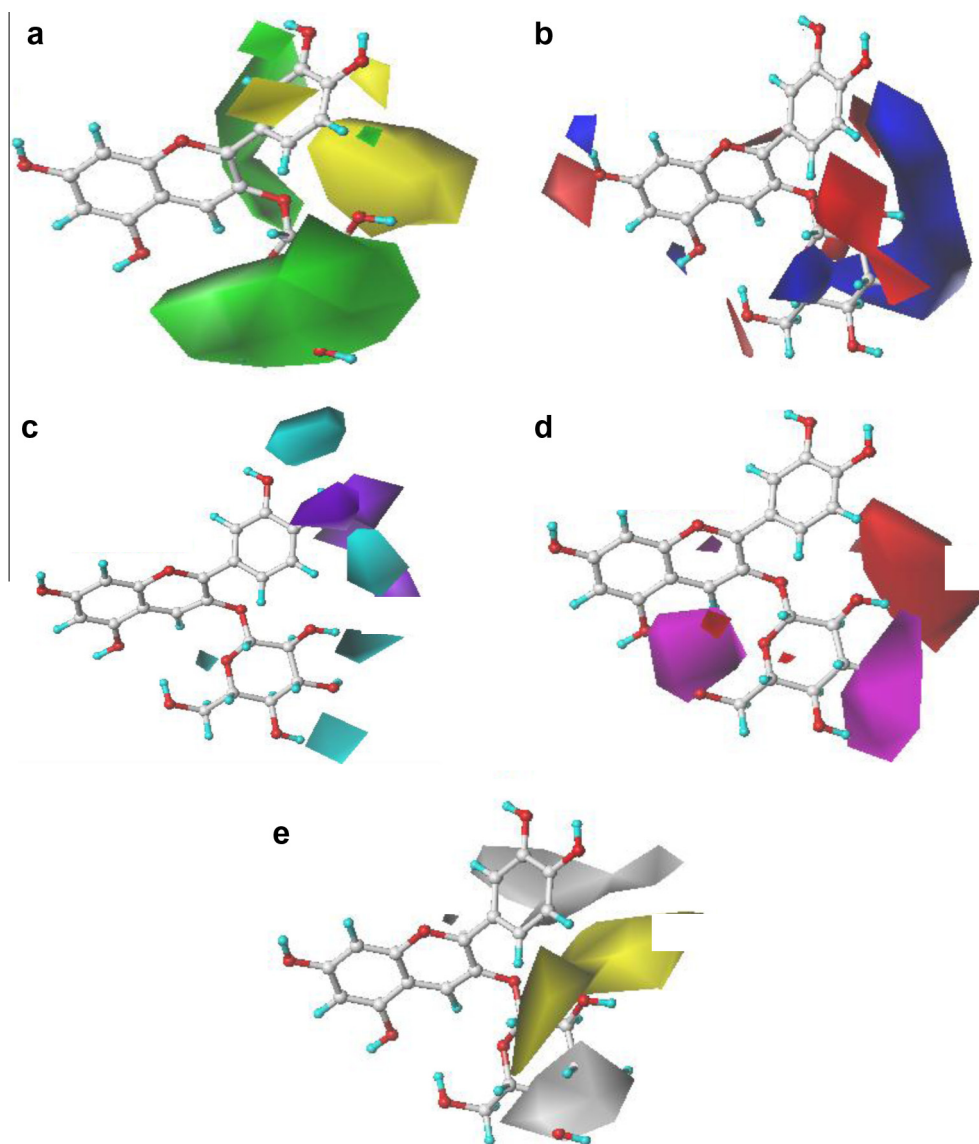


Fig. 3. CoMSIA contour maps. (a) steric contour map: the green is sterically favored for the activity, whereas the yellow is unfavourable; (b) electrostatic contour map: the blue for positive-charged substituent is favourable, whereas the red for the negative-charged substituent is favourable; (c) hydrogen bond donor contour map: the cyan for hydrogen bond donors is favourable whereas the purple for hydrogen bond donors is unfavourable for the activity; (d) hydrogen bond acceptor contour map: the magenta for hydrogen bond acceptors is favourable for the activity whereas the red for hydrogen bond acceptors is unfavourable for the activity; (e) hydrophobic contour map: the yellow for hydrophobic group is favourable whereas the grey for hydrophobic group is unfavourable. (For interpretation of the references to colour in this figure legend, the reader is referred to the web version of this article)

TEAC = 6.764), and compound 17 (R_1 : OCH₃, R_2 : OH, R_3 : H, R_4 : Glc, R_5 : H, TEAC = 5.178) showed higher activity than the corresponding compound 2 (R_1 : H, R_2 : OH, R_3 : H, R_4 : H, R_5 : H, TEAC = 5.801), and compound 4 (R_1 , R_2 : OH, R_3 : H, R_4 : Glc, R_5 : H, TEAC = 4.723), respectively. Therefore, the glycosylation of anthocyanins is important for their antioxidant activity. The glycosides either increased or decreased activity of the aglycons (Kahkonen & Heinonen, 2003). The bulky groups such including glycosyl or acyl groups may contribute to stabilise anthocyanins (Bao et al., 2005).

Fig. 2b shows the electrostatic contour map with electronegative favored (marked in red) and electropositive favored (marked in blue) regions. Two electronegative favored regions in Fig. 2b were located at the 3-position in the C ring, indicating that the presence of an electron-donating group or high electron density on these sites increased the activity. For example, compound 9 (R_1 , R_2 : OH, R_3 : H, R_4 : Rut, R_5 : H, TEAC = 5.940) showed a greater activity than compound 4 (R_1 , R_2 : OH, R_3 : H, R_4 : Glc, R_5 : H,

TEAC = 4.723) due to the number of OH, that is, electron-donating group, at the glycosylation. In addition, another two red contours are located at the R_1 and R_2 position in the B ring, suggesting that electron-donating group or high electron density on these sites is preferred to enhance the antioxidant activity of anthocyanins. For example, compound 1 (R_1 , R_2 : OH, R_3 : H, R_4 : H, R_5 : H, TEAC = 6.764), and compound 17 (R_1 :OCH₃, R_2 : OH, R_3 : H, R_4 : Glc, R_5 : H, TEAC = 5.178) showed a higher activity than the compound 2 (R_1 : H, R_2 : OH, R_3 : H, R_4 : H, R_5 : H, TEAC = 5.801), and compound 4 (R_1 , R_2 : OH, R_3 : H, R_4 : Glc, R_5 : H, TEAC = 4.723), respectively.

3.4. CoMSIA contour maps

The contour maps for the CoMSIA model are shown in Fig. 3. The steric contour map and electrostatic contour map (Fig. 3a and b) are similar to the CoMFA contour map (Fig. 2a and b).

Table 3
Chemical structure and oxygen radical absorbance capacity of anthocyanins from eggplant and radish.

Orgin	Anthocyanins	R1	R2	R3	R4	R5	Predicted TEAC		Experimental	Relative Error (%)	
							CoMFA	CoMSIA		CoMFA	CoMSIA
Eggplant	Dp-3-[(4''-p-coumaroyl)-rham(1→6)glc]-5-glc	OH	OH	OH	O-cou-run	O-glc	4.994	5.238	5.106	2.19	-2.59
	Dp-3-rut-5-glc	OH	OH	OH	O-run	O-glc	4.293	5.166	4.482	4.22	-15.26
	Pg-3-soph-5-glc	H	OH	H	O-sop	O-glc	1.68	0.917	NA	NA	NA
Radish	Pg-3-[(6''-p-coumaroyl)-glc(2→1)glc]-5-(6''-malonyl)-glc	H	OH	H	O-cou-sop	O-malonyl-glc	4.836	4.851	4.921	1.73	1.42

dp, delphinidin; pg, pelargonidin; glc, glucoside; rham, rhamnoside; rut, rutinoside; soph, sophoroside; cou, coumaroyl; mal, malonyl; cou-rut, rutinose acylated with *p*-coumaric acid; cou-sop, sophoroside acylated with *p*-coumaric acid.

Relative error (%) = (experimental value – predicted value)/experimental value × 100%.

NA, not available.

The hydrogen-bond donor and hydrogen-bond acceptor fields in the CoMSIA model are shown in Fig. 3c and d, respectively. The hydrogen-bond donor substituent around the cyan region (R₃-position in the C ring or R₁ position in the B ring), and/or hydrogen bond acceptors around the magenta region (R₃-position in the C ring) should be favourable for the ORAC of anthocyanins. This could be explained by the fact that a hydrogen bond donor in the phenol ring could be convenient for forming intermolecular hydrogen bonds and stabilizing the phenol radicals (Dangles & Fargeix, 2000). The hydroxyl or glycosylation substituent around the cyan region or magenta region should be favourable for high activity since they are both hydrogen bond acceptors and hydrogen bond donors.

Fig. 3e illustrates the CoMSIA hydrophobic contour, where hydrophobic groups in the yellow or grey regions are favourable or unfavourable for the ORAC of anthocyanins, respectively. A large yellow region is located at the R₄ position in the C ring, suggesting that hydrophobic substituents in the region might enhance the activity of anthocyanins.

The developed CoMFA and CoMSIA models could explain structure/activity relationships of most of anthocyanins on the oxygen radical absorbance capacity. Three key points have been concluded on anthocyanin structure–ORAC relationships. Firstly, a bulky and/or electron-donating substituent at the 3-position in the C ring appears to be necessary for enhancing ORAC of anthocyanins based on Fig. 2a and b, or Fig. 3a and b. The conclusion is consistent with the study by Rosso et al. (De Rosso, Moran Vieyra, Mercadante, & Borsarelli, 2008), indicating that the antioxidant activity of anthocyanins is probably due to the steric hindrance effects of bulky glycoside groups. Additionally, the presence of additional electron-donating and/or hydrophobic groups around the glycosylation might enhance the radical scavenging activity (Figs. 1b and 2e), consistent with previous studies (Kahkonen & Heinonen, 2003; Nakajima, Sato, Hoshino, Yamazaki, & Saito, 2006). Lastly, the presence of a hydrogen bond donor group/electron donating group at the R₁ position in the B ring might enhance the radical scavenging activity of anthocyanins based on Figs. 2b, 3c and d, since anthocyanins could act either as hydrogen atom transferers or as electron transferers for their radical scavenging activity (Estevez, Otero, & Mosquera, 2010; Warren, Tronic, & Mayer, 2010).

3.5. Oxygen radical absorbance capacity of anthocyanins from eggplant and radish

Four anthocyanins including pelargonidin-3-sophoroside-5-glucoside, pelargonidin-3-[(6''-p-coumaroyl)-glucosyl(2→1)glucoside]-5-(6''-malonyl)-glucoside, delphinidin-3-rutinoside-5-glucoside, and delphinidin-3-[(4''-p-coumaroyl)-rhamnosyl(1→6)glucoside]-5-glucoside originally from radish and eggplant were randomly chosen to calculate their theoretical TEAC values based on the established CoMFA and CoMSIA models. Their oxygen radical absorbance capacity varied from 0.917 to 5.238 μmol

trolox equivalents (TE)/μmol of anthocyanins in Table 3, whereas anthocyanins except pelargonidin-3-sophoroside-5-glucoside appeared to have high antioxidant power theoretically. The potential anthocyanins including pelargonidin-3-[(6''-p-coumaroyl)-glucosyl(2→1)glucoside]-5-(6''-malonyl)-glucoside, delphinidin-3-rutinoside-5-glucoside, and delphinidin-3-[(4''-p-coumaroyl)-rhamnosyl(1→6)glucoside]-5-glucoside were isolated and then confirmed structurally by Mass and NMR spectrometry. Their experimental ORAC values were shown in Table 3. Except that delphinidin-3-rutinoside-5-glucoside had a high relative error (–15.26%), others were no more than 4.22%.

Their ORAC followed an order: delphinidin-3-[(4''-p-coumaroyl)-rhamnosyl(1→6)glucoside]-5-glucoside > pelargonidin-3-[(6''-p-coumaroyl)-glucosyl(2ucogluco-5-(6''-malonyl)-glucoside > delphinidin-3-rutinoside-5-glucoside.

Delphinidin-3-[(4''-p-coumaroyl)-rhamnosyl(1amngluco-5-glucoside with a bulky substituent at the R₃-position in the C ring and hydrogen bond donor group/electron donating group on the R₁ position in the B ring, whereas pelargonidin-3-[(6''-p-coumaroyl)-glucosyl(2ucogluco-5-(6''-malonyl)-glucoside has a bulky substituent at the R₃-position and delphinidin-3-rutinoside-5-glucoside preserves a hydrogen bond donor group/electron donating group on the R₁ position in the B ring, respectively. The pelargonidin-3-sophoroside-5-glucoside does not satisfy the two structural criteria for a high oxygen radical absorbance capability.

4. Conclusions

The established QSAR models as an effective tool were allowed to screen radish/eggplant anthocyanins for their high oxygen radical absorbance activity (ORAC) so that potential anthocyanins were isolated from radish/eggplant and confirmed experimentally. The structural criteria for anthocyanins with high ORAC based on CoMFA and CoMSIA models could provide deeper insight into the mechanisms of their radical scavenging activities.

Acknowledgments

This study was funded by the National Nature Science Foundation of China (Grant No. 31071530), and the Young Scientist foundation from School of Agriculture and Biology, Shanghai Jiao Tong University (Grant No. NQN201009).

Appendix A. Supplementary data

Supplementary data associated with this article can be found, in the online version, at <http://dx.doi.org/10.1016/j.foodchem.2013.08.082>.

References

- Azuma, K., Ohyama, A., Ippoushi, K., Ichianagi, T., Takeuchi, A., Saito, T., et al. (2008). Structures and antioxidant activity of anthocyanins in many accessions of eggplant and its related species. *Journal of Agriculture and Food Chemistry*, *56*, 10154–10159.
- Bao, J., Cai, Y., Sun, M., Wang, G., & Corke, H. (2005). Anthocyanins, flavonols, and free radical scavenging activity of Chinese bayberry (*Myrica rubra*) extracts and their color properties and stability. *Journal of Agriculture and Food Chemistry*, *53*, 2327–2332.
- Bush, B. L., & Nachbar, R. B. Jr. (1993). Sample-distance partial least squares: PLS optimized for many variables, with application to CoMFA. *Journal of Computer-Aided Molecular Design*, *7*, 587–619.
- Clark, M., Cramer, R. D., & Vanopdenbosch, N. (1989). Validation of the general purpose Tripos 5.2 force field. *Journal of Computational Chemistry*, *10*, 982–1012.
- Cramer, R. D., Patterson, D. E., & Bunce, J. D. (1988). Comparative molecular field analysis. *Journal of the American Chemical Society*, *110*, 1–10.
- Dangles, O., & Fargeix, G. (2000). Antioxidant properties of anthocyanins and tannins: a mechanistic investigation with catechin and the 3',4',7-trihydroxyflavylium ion. *Journal of the Chemical Society-Perkin Transactions*, *2*, 1653–1663.
- De Rosso, V. V., Moran Vieyra, F. E., Mercadante, A. Z., & Borsarelli, C. D. (2008). Singlet oxygen quenching by anthocyanin's flavylium cations. *Free Radical Research*, *42*, 885–891.
- Durst, R. W., & Wrolstad, R. E. (2001). Separation and characterization of anthocyanins by HPLC. In R. E. Wrolstad (Ed.), *Current protocols in food analytical chemistry* (pp. F1.3.1–F1.3.13). NY: John Wiley and Sons, Inc.
- Estevez, L., Otero, N., & Mosquera, R. A. (2010). A computational study on the acidity dependence of radical-scavenging mechanisms of anthocyanidins. *Journal of Physical Chemistry B*, *114*, 9706–9712.
- Golbraikh, A., & Tropsha, A. (2002). Beware of q²! *Journal of Molecular Graphics and Modelling*, *20*, 269–276.
- Ichianagi, T., Kashiwada, Y., Shida, Y., Ikeshiro, Y., Kaneyuki, T., & Konishi, T. (2005). Nasunin from eggplant consists of cis–trans isomers of delphinidin 3-[4-(p-coumaroyl)-L-rhamnosyl(1→6)glucopyranoside]-5-glucopyranoside. *Journal of Agriculture and Food Chemistry*, *53*, 9472–9477.
- Jing, P., Zhao, S. J., Jian, W. J., Qian, B. J., Dong, Y., & Pang, J. (2012). Quantitative studies on structure–DPPH* scavenging activity relationships of food phenolic acids. *Molecules*, *17*, 12910–12924.
- Kahkonen, M. P., & Heinonen, M. (2003). Antioxidant activity of anthocyanins and their aglycons. *Journal of Agriculture and Food Chemistry*, *51*, 628–633.
- Klebe, G., & Abraham, U. (1999). Comparative molecular similarity index analysis (CoMSIA) to study hydrogen-bonding properties and to score combinatorial libraries. *Journal of Computer-Aided Molecular Design*, *13*, 1–10.
- Kong, J. M., Chia, L. S., Goh, N. K., Chia, T. F., & Brouillard, R. (2003). Analysis and biological activities of anthocyanins. *Phytochemistry*, *64*, 923–933.
- Moore, J., Hao, Z., Zhou, K., Luther, M., Costa, J., & Yu, L. L. (2005). Carotenoid, tocopherol, phenolic acid, and antioxidant properties of Maryland-grown soft wheat. *Journal of Agriculture and Food Chemistry*, *53*, 6649–6657.
- Nakajima, J., Sato, Y., Hoshino, T., Yamazaki, M., & Saito, K. (2006). Mechanistic study on the oxidation of anthocyanidin synthase by quantum mechanical calculation. *Journal of Biological Chemistry*, *281*, 21387–21398.
- Noda, Y., Kneyuki, T., Igarashi, K., Mori, A., & Packer, L. (2000). Antioxidant activity of nasunin, an anthocyanin in eggplant peels. *Toxicology*, *148*, 119–123.
- Rahman, M. M., Ichianagi, T., Komiyama, T., Hatano, Y., & Konishi, T. (2006). Superoxide radical- and peroxynitrite-scavenging activity of anthocyanins; structure–activity relationship and their synergism. *Free Radical Research*, *40*, 993–1002.
- Rice-Evans, C., Miller, N. J., & Paganga, G. (1996). Structure–antioxidant activity relationships of flavonoids and phenolic acids. *Free Radical Biology & Medicine*, *20*, 933–956.
- Seeram, N. P., & Nair, M. G. (2002). Inhibition of lipid peroxidation and structure–activity-related studies of the dietary constituents anthocyanins, anthocyanidins, and catechins. *Journal of Agriculture and Food Chemistry*, *50*, 5308–5312.
- Vajragupta, O., Boonchoong, P., & Wongkrajang, Y. (2000). Comparative quantitative structure–activity study of radical scavengers. *Bioorganic & Medicinal Chemistry*, *8*, 2617–2628.
- Wang, H., Cao, G., & Prior, R. L. (1997). Oxygen radical absorbing capacity of anthocyanins. *Journal of Agriculture and Food Chemistry*, *45*, 304–309.
- Wang, H., Nair, M. G., Strasburg, G. M., Chang, Y. C., Booren, A. M., Gray, J. I., et al. (1999). Antioxidant and anti-inflammatory activities of anthocyanins and their aglycon, cyanidin, from tart cherries. *Journal of Natural Products*, *62*, 294–296.
- Warren, J. J., Tronic, T. A., & Mayer, J. M. (2010). Thermochemistry of proton-coupled electron transfer reagents and its implications. *Chemical Reviews*, *110*, 6961–7001.
- Yamagami, C., Akamatsu, M., Motohashi, N., Hamada, S., & Tanahashi, T. (2005). Quantitative structure–activity relationship studies for antioxidant hydroxybenzalacetones by quantum chemical- and 3-D-QSAR(CoMFA) analyses. *Bioorganic & Medicinal Chemistry Letters*, *15*, 2845–2850.
- Yoshiki, Y., Okubo, K., & Igarashi, K. (1995). Chemiluminescence of anthocyanins in the presence of acetaldehyde and tert-butyl hydroperoxide. *Journal of Bioluminescence and Chemiluminescence*, *10*, 335–338.
- Zhang, L., Tsai, K. C., Du, L., Fang, H., Li, M., & Xu, W. (2011). How to generate reliable and predictive CoMFA models. *Current Medicinal Chemistry*, *18*, 1–8.